Particle dynamics in multistage wakefield collider

S. Cheshkov, T. Tajima,* and W. Horton
Department of Physics and Institute for Fusion Studies, The University of Texas at Austin, Austin, Texas 78712

K. Yokoya
KEK National Laboratory for High Energy Physics, Tsukuba-Shi, Japan
(Received 24 January 2000; published 27 July 2000)

The dynamics of particles in laser pulse-driven wakefields over multistages in a collider is studied. A map of phase space dynamics over a stage of wakefield acceleration induced by a laser pulse (or electron beam) is derived. The entire system of a collider is generated with a product of multiple maps of wakefields, drifts, magnets, etc. This systems map may include offsets of various elements of the accelerator, representing noise and errors arising from the operation of such a complex device. We find that an unmitigated strong focusing of the wakefield coupled with the alignment errors of the position (or laser beam aiming) of each wakefield stage and the unavoidable dispersion in individual particle betatron frequencies leads to a phase space mixing and causes a transverse emittance degradation. The rate of the emittance increase is proportional to the number of stages, the energy of the particles, the betatron frequency, the square of the misalignment amplitude, and the square of the betatron phase shift over a single stage. The accelerator with a weakened focus in a channel can, therefore, largely suppress the emittance degradation due to errors.

PACS numbers: 52.40.Nk, 52.65.Cc, 52.75.Di, 05.40.–a

I. INTRODUCTION

The use of plasma waves excited by laser beams for electron acceleration was proposed by Tajima and Dawson [1]. Many variants of this are currently under consideration: plasma beat wave accelerator (PBWA), laser wakefield accelerator (LWFA), and plasma wakefield accelerator (PWFA). These schemes are to excite the wakefield or accelerating structure based on different ways, but the basic idea is common. Thus, a common mathematical treatment of the acceleration process is possible when it is considered as an element of a system of a large scale high energy accelerator. Existing designs [2] of e^+e^- accelerators based on conventional technology aim at a center-of-mass energy of up to 1 TeV. However, to reach higher energy frontiers new acceleration methods seem to be needed. The feature of plasma based accelerators (for a review see [3]) is their ability to sustain extremely large acceleration gradients ($\sim$100 GV/m). In principle, it means several orders of magnitude higher energy gain than the ones achieved by rf technology. For an accelerator in high energy physics, the energy is one of the important parameters, but many others are also crucial for such an accelerator. Since the decrease of cross sections is generally inversely proportional to the energy of the beams, high luminosity is required to detect new physics. The requirement for luminosity, in turn, demands for low beam emittance. The geometrical luminosity is given by

$$\mathcal{L} = \frac{f_c N^2}{4\pi\sigma_x\sigma_y} = \frac{\gamma f_c N^2}{4\pi\sqrt{\epsilon_x\beta_x^*}\sqrt{\epsilon_y\beta_y^*}}, \qquad (1)$$

where f_c is the collision frequency, N is the particle number per bunch, σ_x and σ_y are the rms beam sizes at the interaction point (IP), β_x^* and β_y^* are the betatron lengths at the IP, and ϵ_x and ϵ_y are the normalized transverse emittances of the beams. Thus, the analysis of the performance of laser wakefield accelerators should consider all relevant beam parameters, such as emittance, in addition to the beam energy [4]. Emittance is the measure of the phase space volume of the beam so that it is directly related to the entropy of the beam (through a logarithm). A complex system of a collider, such as the laser wakefield collider, is bound to generate entropy over multiple stages of acceleration. Thus, the understanding of the emittance degradation and possible ways to suppress it is of principal importance.

The essence of mathematics is to extract a map from the particle dynamics in phase space over one stage and then to multiply over as many elements as there are in the system to yield the final overall map. The properties of this map are generically the same for many schemes of the wakefield based accelerators, as mentioned above. We first derive the ideal map in which no disturbance or noise is present in each element of the accelerator. We survey the mathematical properties of the ideal map. Then we go on to study a realistic or nonideal map in which the disturbance or noise of the system such as the ground shake, plasma noise, collisions, laser misalignment, etc. is incorporated. To make our discussion concrete, we take in most of our discussions the example of laser wakefield, following the approach described in [5,6].

*Also at Lawrence Livermore National Laboratory, Livermore, CA 94550.

We note that with a short pulse laser driver the whole acceleration process takes place over a period too short for plasma ions to move. Therefore the analysis is limited to considering electron motion only in a background of immobile ions. This not only simplifies the analysis, but (generally speaking) stabilizes the system. In most scenarios the desired final energy of accelerating particles (~TeV) cannot be achieved over a single acceleration stage. Thus we need to evaluate the effects associated with multistaging and analyze the complete acceleration process. In the present investigation we limit ourselves to the linear regime of wakefield generation.

A major simplification arises from the separate treatment of beam electrons and plasma electrons. The plasma electrons are supporting the wakefield but not trapped by it. On the other hand, the beam electrons are affected (accelerated and focused) by the wakefield. To formulate our map approach, we need analytical expressions for the wakefields in homogeneous plasma for the ideal case. Following [7] we obtain the longitudinal and radial wakefields in the case of cylindrical geometry. Several simplifying assumptions valid in the ultrarelativistic case allow us to integrate the single particle motion for the accelerated beam particles. Based on these results, we derive a map for a multistage LWFA which is used as a base for orbital tracking in Sec. III. In Sec. IV we introduce random errors in the accelerator stage alignment. We consider their effects on the transverse rms beam emittance over multiple stages through our map code for different conditions. These errors combined with the spread in individual particle betatron frequencies can lead to a considerable emittance growth. To understand, optimize, and improve the performance of the LWFA based collider, it is necessary to study the statistical mechanics behavior of these particle dynamics. From this we obtain analytical expressions of emittance degradation in the accelerator map in Sec. V. The case with mitigated focusing force is discussed in Sec. VI to alleviate the emittance degradation. Conclusions are drawn in Sec. VII.

II. WAKEFIELD MODEL

A short high power laser pulse propagating in plasma can excite wakefields. The plasma response can be obtained from the cold fluid equations [7]:

$$\frac{d}{dt}\,\mathbf{v} = -\frac{e}{m_e\gamma}\left[\mathbf{E} + \frac{1}{c}\,\mathbf{v}\times\mathbf{B} - \frac{1}{c^2}\,\mathbf{v}(\mathbf{v}\cdot\mathbf{E})\right], \quad (2)$$

$$\frac{\partial}{\partial t}\,n + \nabla\cdot n\mathbf{v} = 0\,, \quad (3)$$

where n is the electron density and γ is the Lorenz factor. These equations may be solved perturbatively, assuming that the density perturbation is relatively small. In the leading order the motion of the plasma electrons is governed by the ponderomotive force

$$\mathbf{F} = e\nabla\Phi_l(r,z,t)\,, \quad (4)$$

where the ponderomotive potential Φ_l is related to the laser vector potential A_l,

$$\Phi_l(r,z,t) = -\frac{m_e c^2}{2e}\,a_0^2(r,z,t)\,, \qquad a_0 = \frac{eA_l}{m_e c^2}\,, \quad (5)$$

and a_0 is the normalized vector potential.

Using a Gaussian laser pulse of the form (with a pulse length l_l, spot size r_s)

$$\mathbf{A}_1 = \mathbf{A}_{10}\exp\left(-\frac{\xi^2}{2l_l^2}\right)\exp\left(-\frac{r^2}{r_s^2}\right), \quad (6)$$

where $\xi = z - v_g t$ and the group velocity v_g is very close to the speed of light and the maximum electric field in the z direction, behind the pulse ($\xi^2 \gg l_l^2$), is

$$E_z(\xi,r) = -a_0^2\sqrt{\frac{\pi}{2e}}\,E_0\exp\left(-\frac{2r^2}{r_s^2}\right)\cos k_p\xi\,, \quad (7)$$

where $E_0 = \frac{m_e w_p c}{e}$ is the so-called wave breaking field and we used the approach of [8]. The maximum field (7) is reached when the resonance condition [3] is satisfied: $l_l = \lambda_p/(\pi\sqrt{2})$, where λ_p is the plasma wave wavelength $2\pi c/\omega_p$. A transverse electric field E_r and magnetic field B_θ are generated according to the Panofski-Wenzel theorem [9],

$$\frac{\partial E_z}{\partial r} = \frac{\partial(E_r - B_\theta)}{\partial\xi}\,, \quad (8)$$

leading to

$$(E_r - B_\theta) = 4\,\frac{a_0^2}{r_s^2}\sqrt{\frac{\pi}{2e}}\,\frac{E_0}{k_p}\,r\exp\left(-\frac{2r^2}{r_s^2}\right)\sin k_p\xi\,. \quad (9)$$

For a relativistic particle ($v_z \approx c$) the transverse force is proportional to $(E_r - B_\theta)$ and there is a region in the wake (quarter period) where a relativistic electron experiences simultaneous acceleration and focusing. This feature of the LWFA makes it different from the conventional accelerators. The wakefield structure of this model is common to other sisters of wakefield accelerators such as PBWA and PWFA (see, for example, [10]). In general, it is a typical feature of plasma based accelerators that the accelerating field is independent of the transverse coordinates (up to second order) and the focusing force is linear in transverse coordinates (up to third order):

$$E_z \propto \cos\Psi, \qquad E_r - B_\theta \propto r\sin\Psi\,. \quad (10)$$

We assume that we have an electron injector which can be used as a charged particle source for our accelerator. Designing such an injector is a task in itself (see, e.g., [11–13]), but we are not going to investigate it here. Motion of the high energy electrons of the beam in the plasma wakefield is analyzed based on the following assumptions: (i) The phase space area occupied by the

beam particles is small; (ii) the wakefield is not affected by the beam (however, the beam loading can be included [6]); (iii) the particles in the beam are highly relativistic and move predominantly in the z direction (which is the direction of propagation of the laser pulse),

$$\dot{z} \gg \dot{x}, \dot{y}, \qquad \dot{z} \approx c\,;$$

(iv) the particle motions in x and y are decoupled and can be considered independently; (v) there is no interaction among the beam particles; and (vi) the laser pulse does not evolve. It is important, however, to ascertain mathematical and physical properties of a simplified accelerator system first in order to isolate and gain insight into the essential mechanism of the emittance degradation. To lift some of these assumptions is relatively straightforward and work in progress on the problem will relax some of them. The wakefield generated by the beam can be included in the considerations using the results in [14]. Assumption (v) is justified for high energy particles and relatively low currents, because the space charge force diminishes by a factor of $1/\gamma^2$. Assumption (vi) is related to the pump-depletion problem [15] and will be taken into account in the future.

Starting with the single particle equation of motion $\frac{d\mathbf{p}}{dt} = -e(\mathbf{E} + \frac{\mathbf{v}\times\mathbf{B}}{c})$ and assuming that the beam particles are close to the z axis, we obtain the following basic system of differential equations for the longitudinal motion:

$$\frac{d\gamma}{dz} = k_p \Phi_0 \cos\Psi\,, \tag{11}$$

$$\frac{d\Psi}{dz} = k_p\left(1 - \frac{\beta_p}{\beta}\right), \tag{12}$$

where $\Psi = k_p\, z - \omega_p\, t(z)$ is the particle phase with respect to the wakefield. For the transverse motion

$$\frac{d\hat{p}_u}{dz} = -\frac{4\Phi_0}{r_s^2}\,\hat{u}\sin\Psi\,, \tag{13}$$

$$\frac{d\hat{u}}{dz} = \frac{\hat{p}_u}{\gamma}\,, \tag{14}$$

where

$$\beta_p = v_p/c, \qquad \Phi_0 = \sqrt{\frac{\pi}{2e}}\,a_0^2\,, \tag{15}$$

$$\hat{u} = u, \qquad \hat{p} = \frac{p_u}{m_e c}\,. \tag{16}$$

Here $E_0 = cm_0\omega_p/e$, $k_p = \omega_p/c$, v_p is the phase velocity of the wake and u and p_u stand for transverse variables x and p_x or y and p_y. After convenient normalizations, the important points are that we use z as our time coordinate and the energy and phase of the particles with respect to the wake are our "longitudinal" variables. Equations (11) and (12) decouple from (13) and (14), and we can consider these two sets independently. The first set is conveniently analyzed using the following one-dimensional Hamiltonian [16]:

$$H = k_p\gamma(1 - \beta\beta_p) + k_p\Phi(\Psi)\,, \tag{17}$$

where

$$\Phi(\Psi) = -\Phi_0 \sin\Psi\,. \tag{18}$$

In the phase space formed by the first pair of variables (γ, Ψ) we have stable fixed points, $\gamma = \gamma_p$ and $\Psi = \pi/2 + 2n\pi$, and unstable fixed points, $\gamma = \gamma_p$ and $\Psi = -\pi/2 + 2n\pi$, where $\gamma_p = 1/\sqrt{1 - \beta_p^2}$ is the Lorenz factor corresponding to the phase velocity of the plasma wave. There are two phase space regions—the trapped region, where the particles execute bounded motion, and the untrapped one, where the motion is unbounded in the Ψ direction (see Fig. 1). Because we are primarily interested in high energy physics applications of LWFA here, we consider the untrapped case, where the particle orbits are well above the separatrix. We can further simplify the equations of motion for γ and Ψ by putting $\beta = 1$ for ultrahigh energy particles to obtain

$$\frac{d\gamma}{dz} = k_p\Phi_0\cos(\Psi)\,, \tag{19}$$

$$\frac{d\Psi}{dz} = \frac{k_p}{2\gamma_p^2}\,. \tag{20}$$

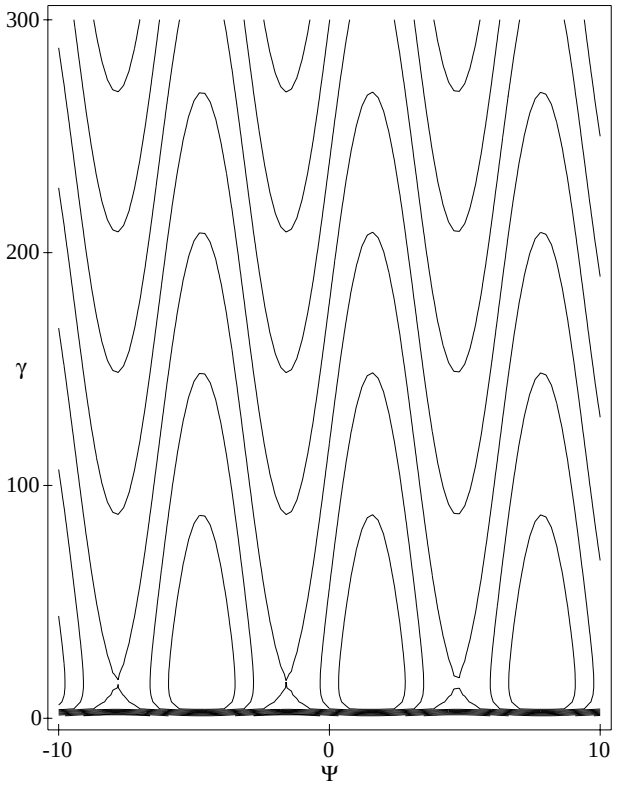

FIG. 1. The longitudinal phase space: electron Lorenz factor γ vs its phase with respect to the wakefield Ψ. The parameters used were $\gamma_p = 15$, $\Phi_0 = 0.2$.

These equations are integrated directly to give

$$\Delta\gamma = 2\Phi_0\gamma_p^2(\sin\Psi - \sin\Psi_0)\,, \tag{21}$$

$$\Psi = \Psi_0 + \frac{k_p z}{2\gamma_p^2}\,, \tag{22}$$

where Ψ_0 is the initial phase of the particle with respect to the wakefield. First, we observe that the maximum energy gain in (21) is $2\Phi_0\gamma_p^2$. We call this an energy gain per unit stage. In order to gain more energy, we need multiple stages. Taking typical values of the parameters $\Phi_0 = 0.2$ (which corresponds to $a_0 = 0.5$, corresponding to the intensity of about 3×10^{17} W/cm^2 for 1 μm laser wavelength) and $\gamma_p = 100$ we see that the above gain is about 4×10^3 in units of electron's rest energy, or about 2 GeV. This energy is achieved over a distance z of about 50 cm. We take $a = 0.5$ to be still in the "controlled" linear regime. The actual gain is smaller if the pump depletion [15] is taken into account. Last, we note that by properly choosing Φ_0, r_s, and γ_p we can analyze other plasma based accelerators, e.g., PWFA.

III. MULTISTAGE ACCELERATION AND THE MAP

If we are to accelerate particles to TeV energies, we need to investigate problems associated with the multistaging. Such a design based on the LWFA acceleration method has been devised in [4] to satisfy all the known accelerator physics constraints. In order to analyze the properties and efficacy of the so-designed accelerator we characterize the beam dynamics to obtain a map which describes the one-to-one correspondence between the entrance phase space coordinates and the exit coordinates of the beam particles during the propagation of the beam through each accelerating stage and concatenate these maps over many stages. We use the multiple product of maps to build a systems code for a LWFA collider. As in the standard rf linac theory [17,18], we have a reference particle moving along the ideal (design) orbit. All other particles in the bunch are described by their relative position with respect to the reference particle.

The linearized equations of motion for the longitudinal degrees of freedom are

$$\delta\Psi_{n+1} = \delta\Psi_n\,, \tag{23}$$

$$\delta\gamma_{n+1} = 2\gamma_p^2\Phi_0[\cos(\Psi_s + \Delta) - \cos(\Psi_s)]\delta\Psi_n + \delta\gamma_n\,, \tag{24}$$

where the subscript n enumerates the stage (n the entrance and $n + 1$ the exit), Ψ_s is the "synchronous" phase, and Δ is the phase slippage per accelerating stage (actually, it can also depend on n). Because of the fact that we are considering extremely high energy particles ($\gamma \sim 10^5$–10^7), the equation (23) is decoupled from (24). Formally, the equations look the same as in standard linac theory when the synchrotron oscillation frequency approaches zero. However, the physical regime of operation for the LWFA is different from the rf linac—we have a significant phase slippage over a stage (it is precisely this slippage which gives us the energy gain)—and it also limits the maximum possible gain per stage. This difference comes from the fact that the plasma wave is relatively slow ($\gamma_p \approx 100$, instead of ∞). For the PWFA, however, the Lorenz factor of the driver can be much higher (for instance, the current Stanford linear collider beam energy [2] corresponds to a Lorenz factor of about 10^5) and then the dephasing is not significant. From Eqs. (23) and (24) we see that, in the approximation we are working in, the phases of the particles do not change and the absolute energy spread increases linearly with the stage number (actually, this is the beginning of a very slow synchrotron oscillation which happens on a time scale much greater than the time it takes a particle to travel the whole accelerator).

Now let us consider the transverse motion. If we assume that the particle energy does not change significantly over a single stage (which is valid in our case), this motion is described by

$$\ddot{\tilde{u}} + \left[\omega_\beta^2 \sin(\omega_s z + \Psi_s + \delta\Psi_n) - \frac{1}{2}\frac{\ddot{\gamma}}{\gamma} + \frac{1}{4}\frac{\dot{\gamma}^2}{\gamma^2}\right]\tilde{u} = 0\,, \tag{25}$$

where

$$\omega_s = \frac{k_p}{2\gamma_p^2}\,, \tag{26}$$

$$\omega_\beta = \left(\frac{4\Phi_0}{\gamma r_s^2}\right)^{1/2} \tag{27}$$

are the "slippage" and maximum betatron frequencies, respectively, in units of $1/m$, and $\tilde{u} = \sqrt{\gamma}\,u$. In the high energy regime the third term in the square brackets in (25) is negligible and the second term is usually also small because of the proportionality to $1/\gamma_p^2$. Still, in the cases of very weak focusing we have to take it into account (for instance, in plasma channel).

An analytic solution can be found when some additional approximations are made. The simplest and first thing to do is to approximate the sine function in (25) by some constant value (known as the "smooth" approximation) and then the equation describes just a simple harmonic oscillator. We adopt this. We also assume a free drift (in vacuum) of the particles between the stages. Let us forget for a moment that the particles are being accelerated and that the strength of the focusing force actually depends on the stage even if the stages are physically identical. To get stable solutions, we need to satisfy

$$|\mathrm{Tr}M| < 2\,, \tag{28}$$

where M is the transfer matrix:

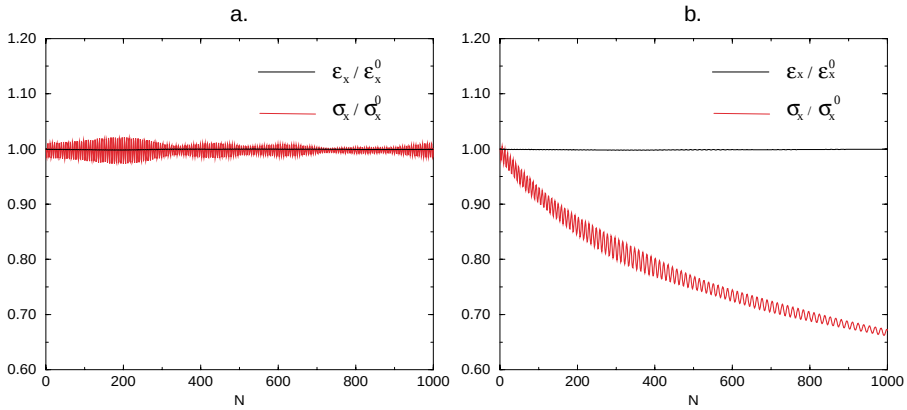

FIG. 2. (Color) The rms beam size σ_x and normalized rms x emittance ϵ_x vs stage number N. The parameters used were $\gamma_p = 100$, drift $= 17$ cm, $\epsilon_x^0 = 2.2$ nm, $r_s = 0.5$ mm, $\sigma_{\delta\gamma}/\gamma = 0.01$, and $\sigma_{\delta\Psi} = 0.01$. (a) No acceleration and no dislocations, (b) no dislocations.

$$M = \begin{pmatrix} \cos(\frac{\omega}{\omega_s}\Delta) & \frac{1}{\omega}\sin(\frac{\omega}{\omega_s}\Delta) \\ -\omega\sin(\frac{\omega}{\omega_s}\Delta) & \cos(\frac{\omega}{\omega_s}\Delta) \end{pmatrix} \begin{pmatrix} 1 & L \\ 0 & 1 \end{pmatrix}, \quad (29)$$

where L is the drift distance between the wakefield stages and $1/\omega$ is the betatron length in the wakefield. The matrix (29) may be also written as

$$M = \begin{pmatrix} \cos(\frac{\omega}{\omega_s}\Delta) & \frac{1}{\omega}\sin(\frac{\omega}{\omega_s}\Delta) + L\cos(\frac{\omega}{\omega_s}\Delta) \\ -\omega\sin(\frac{\omega}{\omega_s}\Delta) & -L\omega\sin(\frac{\omega}{\omega_s}\Delta) + \cos(\frac{\omega}{\omega_s}\Delta) \end{pmatrix}. \quad (30)$$

The transverse map $\mathcal{M}$ for the whole accelerator system is

$$\mathcal{M} = M^N, \quad (31)$$

where N is the total number of stages when each stage has identical physical parameters.

When we do not have any drift space, the solutions of orbits are always stable. If we increase L, keeping the other parameters fixed, at some point we encounter a "blowup" of the amplitude of the betatron oscillations. So the maximum distance between the stages is limited. The trace of M is

$$\mathrm{Tr}M = 2\cos\left(\frac{\omega}{\omega_s}\Delta\right) - \omega L\sin\left(\frac{\omega}{\omega_s}\Delta\right), \quad (32)$$

and for stability it should satisfy (28). We constructed the map code (31). The relation (28) is used to check the map code. Up to some value of L the motion is stable (see Fig. 2a), and after that we indeed find the amplitude blowup. This consideration does not take into account the fact that particles accelerate and ω_β is decreasing ($\omega_\beta \propto \frac{1}{\sqrt{\gamma}}$). Also, in reality, particles have different (random) energies and different (random) phases with respect to the wakefield. Therefore, the above analysis should be carried out for each particle separately, but, if the differences in their phases are small, the conditions for stable motion are practically the same for all the particles. In general,

$$\mathcal{M} = M_N M_{N-1} \cdots M_2 M_1, \quad (33)$$

where the transfer matrices depend on the stage number and the positions of the individual particles in the longitudinal phase space. We note that, because of the common structure of the wakefield in all plasma based accelerators, the obtained map with just slight modifications can be used to analyze their performance as well. We coded the map in the case (33). In [4] three sets of scenarios for 5 TeV collider parameters are presented (see also Table I). Case I calls for the tightest emittance, with the least driver power. We take this case for most of the time as a concrete example. We also assume that the accelerated beam is initially matched to the focusing channel of the accelerator. Our runs show that when we start with a normalized emittance of $\epsilon_u = \epsilon_x = 2.2$ nm (the case I scenario of [4]), up to some value of the drift space the normalized rms emittance is well preserved (see Fig. 2b) and the transverse particle motion is stable. This does not surprise us because the map is volume preserving, so the phase space area (emittance) is constant.

TABLE I. The 5 TeV e^+e^-, $\mathcal{L}_g = 10^{35}$ cm^{-2}s^{-1} collider parameters according to [4].

Case	P_b (MW)	N (10^8)	f_c (kHz)	ϵ_x (nm)	β_x^* (μm)	σ_x (nm)	σ_z (μm)
I	2	0.5	50	2.2	22	0.1	0.32
II	20	1.6	156	25	62	0.56	1
III	200	6	416	310	188	3.5	2.8

IV. ALIGNMENT ERRORS

For a complex system, cumulative errors can give rise to an unpleasant result such as emittance dilution. We identify that one of the most important such effects stems from the alignment errors by whatever mechanism of the wakefield with respect to the design particle orbit stage by stage. The problem here is that up to this point we have not considered possible misalignments of the consequent stages. This, combined with the fact that the focusing force is different for different particles, can lead to a severe transverse emittance growth. Basically, what happens is that the particles rotate at different angular velocities in the transverse phase space and, if there is a stage position shift present, we get a characteristic banana-shaped distribution (see Fig. 3c) (it is banana shaped only if the dislocation size is larger than the beam size, but in any case the particle distribution gets diluted because of the misalignments). This process critically depends on the magnitude of the betatron frequency spread. This means that the typical strength of the focusing force is of great importance. Of course, additional information can be extracted from the other total phase space cross sections; see Fig. 4. However, here we concentrate on the transverse emittance as a figure of merit due to its importance to the final luminosity of the collider. The effect of plasma noise (or other noise, such as laser or the boundary) on the particle dynamics over a stage may also be incorporated in a map similar to the stage-by-stage alignment errors. Such dynamics results in a fuzzy or stochastic [19] map. The longitudinal stage errors may be incorporated in a similar manner; preliminary analysis shows that their importance is not so critical.

We consider the case of transverse stage misalignments. The dislocation of the aligned position of each stage n is given in our code as a stochastic variable $\mathcal{D}_n$ which we impose to have a Gaussian distribution with zero mean and standard deviation $\sigma_{\mathcal{D}}$ which we assume to be independent of the stage number

$$\begin{pmatrix} \tilde{x}_{n+1} \\ \dot{\tilde{x}}_{n+1} \end{pmatrix} = M_n \begin{pmatrix} \tilde{x}_n - \tilde{\mathcal{D}}_n \\ \dot{\tilde{x}}_n \end{pmatrix} + \begin{pmatrix} \tilde{\mathcal{D}}_n \\ 0 \end{pmatrix}, \tag{34}$$

where $\mathcal{D}_n$ is the stochastic misalignment ($\tilde{\mathcal{D}}_n = \sqrt{\gamma_n}\,\mathcal{D}_n$). The longitudinal degrees of freedom are not affected. For this map to describe realistically the electron motion, we assume that $\sigma_{\mathcal{D}} \ll r_s$. The total transverse map (in the presence of errors) can be written in the form

$$\begin{aligned} \begin{pmatrix} \tilde{x}_{n+1} \\ \dot{\tilde{x}}_{n+1} \end{pmatrix} &= M_n M_{n-1} \cdots M_2 (1 - M_1) \begin{pmatrix} \tilde{\mathcal{D}}_1 \\ 0 \end{pmatrix} \\ &\quad + \cdots (1 - M_n) \begin{pmatrix} \tilde{\mathcal{D}}_n \\ 0 \end{pmatrix} \\ &\quad + M_n M_{n-1} \cdots M_1 \begin{pmatrix} \tilde{x}_1 \\ \dot{\tilde{x}}_1 \end{pmatrix}. \end{aligned} \tag{35}$$

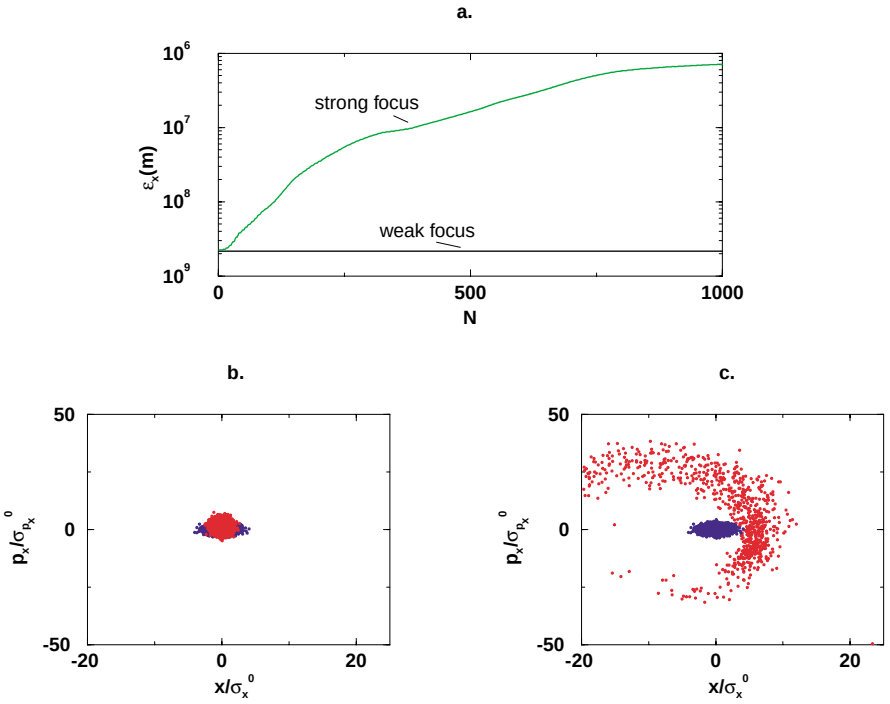

FIG. 3. (Color) Weak and strong focusing cases: (a) The normalized x emittance ϵ_x vs stage number N. The parameters used for the strong focus case were $\gamma_p = 100$, drift = 17 cm, $\epsilon_x^0 = 2.2$ nm, $r_s = 0.5$ mm, $\sigma_{\mathcal{D}} = 0.1\mu$, $\sigma_\gamma/\gamma = 0.01$, and $\sigma_{\delta\Psi} = 0.01$. For the weak focus case see Sec. VI. (b) The phase space p_x vs x for the weak focus case. (c) The strong focus case. The initial (in blue) distribution (Gaussian and the beam is assumed initially matched to the focusing properties of the channel) and the final (in red) after 1000 acceleration stages.

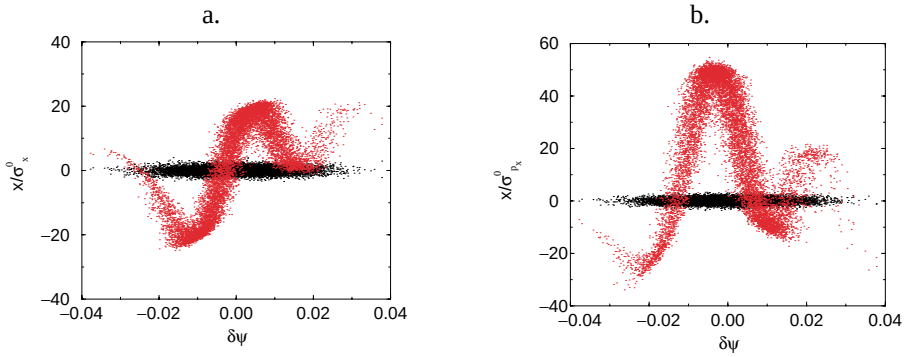

FIG. 4. (Color) Additional cross sections of the initial (black) and final (red) phase space: (a) transverse coordinate vs longitudinal phase, (b) transverse momentum vs longitudinal phase.

V. EMITTANCE DEGRADATION

The stochastic map (35) leads to a transverse emittance degradation. A run with small random dislocations of magnitude $\sigma_{\mathcal{D}} = 1 \times 10^{-7}$ m is presented in Figs. 3a and 3c. We see that in this case (corresponds to design I in [4]) we have a severe emittance growth (the initial normalized emittance is 2.2 nm). Additional results can be found in [5,6]. We have to point out that, even though there are cases corresponding to large laser spot sizes which preserve the normalized emittance quite well, their practical realization would require a huge laser power probably well above any future experimental limits. Some alternative approaches to reduce the emittance growth are discussed in [5,6]. In general, the problem can be cured by decreasing the focusing of the accelerator system. One possible way is to use a plasma channel [20,21]. It provides a linear weak focusing, and we showed in [6] that its performance in a collider application is promising. In Sec. VI we briefly discuss this issue. Here we concentrate on the map properties.

We observe a certain random feature over shorter time scales; runs with different misalignment distributions (just different sequences, otherwise the same macroscopic properties) give different $\epsilon = \epsilon(N)$ behavior. This is due to the fact that the practical number N is too small with respect to the long-range stationary behavior of the map. Even though the emittance is a cumulative quantity which characterizes the particle ensemble as a whole, it still has a stochastic nature. Only in the limit of large N and long enough transverse phase space mixing the final emittance distribution shrinks and we obtain an approximately deterministic value for a given set of parameters and $\sigma_{\mathcal{D}}$. For large N we observe a typical diffusion process; the emittance growth is linearly proportional to N [it is correct only in a constant energy approximation, in the case of adiabatic energy increase the dependence is more complicated; see (44)].

The dependence of the emittance growth on the betatron frequencies spread is quadratic in the beginning (see Fig. 5c), but if the parameters are such that full phase space mixing occurs,

$$\sigma_{\delta\omega} N l > 2\pi\,, \tag{36}$$

where $\sigma_{\delta\omega}$ is the betatron frequency spread and l is the length of a single stage, then the emittance growth rate is practically independent of the particular value of $\sigma_{\delta\omega}/\omega$. The continuous growth of the emittance is maintained under the presence of betatron frequency spread. In the limit of small betatron frequency ω, namely, $\omega\, l < 1$, and small distance between the stages the map reduces to a stochastic differential equation,

$$\ddot{\tilde{x}} + \omega^2 \tilde{x} = \omega^2 \tilde{\mathcal{D}}\,. \tag{37}$$

The right-hand side of the above equation represents the noise (alignment errors) which drives the oscillation. Considering white noise, we observe

$$\langle \mathcal{D} \rangle = 0\,, \tag{38}$$

$$\langle \mathcal{D}(z_1)\mathcal{D}(z_2)\rangle = \sigma_{\mathcal{D}}^2 l\, \delta(z_1 - z_2)\,. \tag{39}$$

Applying the theory of random walk of a harmonic oscillator driven by a random force, we obtain

$$\langle \tilde{x} \rangle = 0, \qquad \langle \dot{\tilde{x}} \rangle = 0, \qquad \langle \tilde{x}\dot{\tilde{x}} \rangle = 0\,, \tag{40}$$

$$\langle \tilde{x}^2 \rangle = Dz = DNl, \qquad \langle \dot{\tilde{x}}^2 \rangle = D\omega^2 z\,, \tag{41}$$

where the diffusion coefficient D is given by

$$D = \frac{1}{2}\,\gamma\omega^2 l \sigma_{\mathcal{D}}^2\,. \tag{42}$$

We are also assuming that the emittance growth is large (compared to the initial emittance). So, using (40) and (41), we obtain

$$\Delta\epsilon \approx \omega D\, z = \frac{1}{2}\,\gamma\omega(\omega l)^2 \sigma_{\mathcal{D}}^2 N\,. \tag{43}$$

The averages in (40) and (41) are twofold: over the particle ensemble and over the noise realizations. However, in the limit of a significant phase mixing and large N the average over the noise realizations can be dropped (in this limit only $\sigma_{\mathcal{D}}$ is important). The alignment errors introduce randomness in the phase space particle positions upon reentry to the next stage; the differential betatron oscillations mix these positions causing an emittance growth.

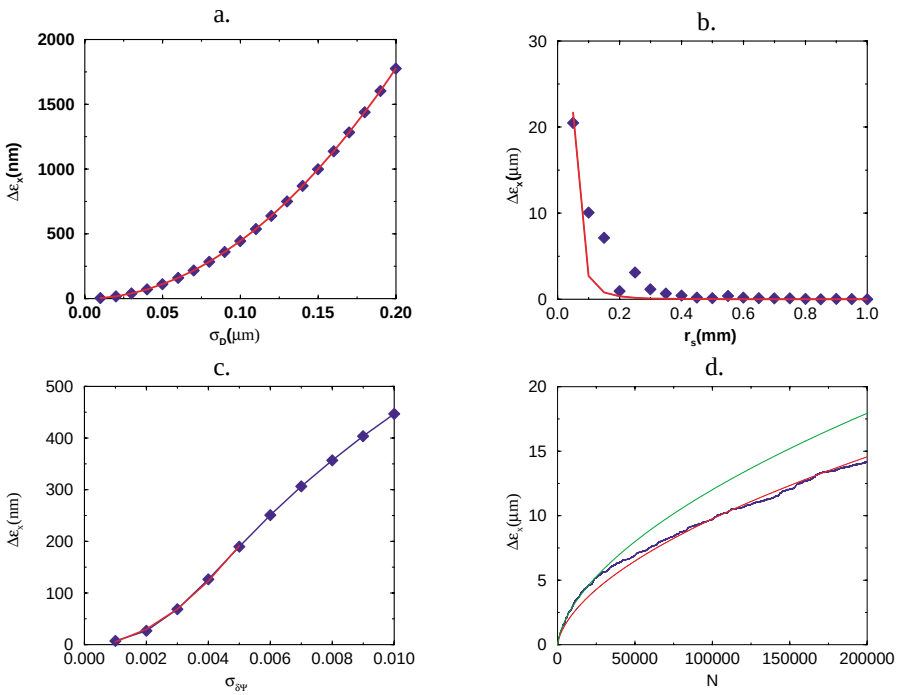

FIG. 5. (Color) Emittance degradation scalings: (a) dependence of the normalized emittance growth $\Delta\epsilon_x$ on the magnitude of the transverse stage offsets $\sigma_{\mathcal{D}}$. Blue diamonds represent the code results and the red line is a quadratic fit. (b) Scaling of the emittance growth with the laser spot radius (which determines the wakefield curvature and, correspondingly, the betatron frequency). The red line is a $1/r_s^3$ [as dictated by (45)] fit to the numerical data (blue diamonds). (c) Scaling of the emittance growth with the phase spread. The change is from quadratic to linear dependence and finally saturation. (d) Long range behavior of the emittance degradation. Two fits to the numerical results (in blue): first (red) based only on the derived N dependence and second (green) based on the complete theoretical prediction.

In fact, the energy increases ($\Delta\gamma$ per stage). In the adiabatic limit we obtain

$$\Delta\epsilon \approx \frac{1}{2}\,\gamma\omega(\omega l)^2\sigma_{\mathcal{D}}^2\left(\frac{\gamma}{\Delta\gamma}\right)^{1/2}\sqrt{N\ln\left(1+\frac{\Delta\gamma N}{\gamma}\right)}, \tag{44}$$

where γ is the initial particle energy. Typically, $\Delta\gamma \approx a_0^2 E_0 l$ and $\omega \propto \frac{a_0}{r_s}$, so we obtain

$$\Delta\epsilon \propto \frac{l^{3/2}a_0^2\sigma_{\mathcal{D}}^2}{r_s^3 E_0^{1/2}}\sqrt{N\ln\left(1+\frac{\Delta\gamma N}{\gamma}\right)}. \tag{45}$$

A very important and expected point is the strong dependence of the emittance growth on the magnitude of the betatron frequency (or wakefield curvature); see Fig. 5b. Discrepancy for small r_s (large betatron frequency) between the numerical and analytical results is caused by violation of our $\omega l < 1$ assumption. Of course, better control of the errors reduces the emittance degradation as shown in Fig. 5a. This important issue will be discussed in a future publication. We can also see from (45) that, for a fixed final energy, reducing the length of a single stage decreases the emittance growth. This point was exploited in Ref. [22]. When the number of stages is relatively small and the phase space mixing is not complete, numerical results appear to be the only reliable way to analyze the properties of the map; analytical estimations are rather difficult. We note that analytical estimations of emittance growth due to stage misalignment valid in the case of full filamentation (phase space mixing) in a single stage can be found in [23]. In this limit (corresponds to a very strong wakefield focusing), control over the emittance growth can be achieved only by precise handling of the beam (namely, error control better than the beam size). The results in this limit can be reproduced in our theory by replacing the factor ωl in (43) by unity.

With the notion of final emittance scaling with the relevant parameters we can start to optimize in the multidimensional parameter space of the future collider. From the computer simulations for the small emittance design [4] for a multi TeV collider, the conclusion is that in the case of initially homogeneous plasma it is difficult to avoid a severe emittance growth of the accelerated beam in the presence of small alignment errors stage-by-stage based on reasonable parameters (laser spot size, dislocation size, and number of stages). The difficulty is primarily due to the fact that the wakefield focusing force is too large in this case. The above considerations do not include the transverse nonlinear effects which also contribute to the emittance increase.

VI. MITIGATED FOCUSING FORCE

A possible way to decrease the wakefield focusing is the "hollow channel" design [20] in which a preformed vacuum channel in an underdense plasma (the overdensed case was studied in [24]) is discussed. This case offers several important advantages: the focusing force is almost exactly (because the phase velocity of the wake mode is very close to the speed of light) linear and weak in the channel (the weak focusing is a very important improvement over that of a uniform plasma case), there exists a stable propagation solution for the laser mode, and the acceleration gradient is very uniform in transverse coordinates within the channel. A drawback is the loss in the magnitude of the accelerating field. The equations for the wakefield in the channel are [20]

$$E_z(\xi, r) = -k_{ch}^2 \int_{\xi}^{\infty} \cos[k_{ch}(\xi - \xi')]\Phi_l(a, \xi')\, d\xi', \tag{46}$$

$$E_r(\xi, r) - B_\theta(\xi, r) = \frac{k_{ch} r}{4\gamma_p^2} k_{ch}^2 \int_{\xi}^{\infty} \sin[k_{ch}(\xi - \xi')]\Phi_l(a, \xi')\, d\xi', \tag{47}$$

where a is the channel radius, Φ_l is the ponderomotive potential, and k_{ch} is given by $k_{ch} = k_p/\sqrt{1 + k_p a \frac{K_0(k_p a)}{2K_1(k_p a)}}$, where K_0 and K_1 are the modified Bessel functions of the zeroth and the first order, respectively. For instance, if we choose $k_p a = 1$ then the electric field in the z direction will be reduced by a factor of 0.6 [20] compared to the initially uniform plasma. So, formally there are no major changes to our previous map scheme. There is a reduction in Φ_0 and the magnitude of the focusing changes,

$$\omega = k_{ch}\left(\frac{\Phi_0}{2\gamma\, \gamma_p^2}\right)^{1/2}.$$

Since the γ_p factor is usually large, the magnitude of the focusing force decreases significantly. We are able to investigate the accelerator performance in this case using the same approach as before.

The run shown in Figs. 3a and 3b indicates a very significant improvement over the previous design. Here we are able to preserve even design I emittance of 2.2 nm. The stage considered is $\gamma_p = 150$, the channel radius $a = 30\ \mu$m, the laser spot size $r_s = 50\ \mu$m, the plasma density (outside the channel) $n = 5 \times 10^{16}\ \mathrm{cm}^{-3}$, the laser wavelength $\lambda \approx 1\ \mu$m, and the drift space is 0.3 m. The magnitude of the stage dislocations is larger than before—$\sigma_{\mathcal{D}} = 0.5\ \mu$m. From the graphs we see that the emittance growth of the accelerated beam is now much smaller and the design is more promising. Unfortunately, there is an additional effect: because in reality we have a finite density gradient it leads to a resonant absorption where the local plasma frequency matches the wakefield frequency. This effect has been studied in [21], where an expression for the quality factor of the hollow channel is derived. Possible low values of this factor limit the acceleration of multiple bunches in a single shot created wakefield.

Another way to decrease the wakefield curvature is through the use of transversely shaped laser pulses. A "flattop" laser pulse would produce a small curvature wakefield and correspondingly small focusing force. Creation and propagation of such pulses needs to be studied. In the case of PWFA the density shaping of the driver electron bunch can be achieved by using octuple magnets.

The most reasonable scenario at present might be the following. We note the results in [25] for monomode laser guiding in a hollow capillary dielectric tube. A femtosecond $10^{16}\ \mathrm{W/cm^2}$ laser pulse is guided over 10 cm with low losses. The transverse intensity profile of such a pulse is $\propto J_0^2(\alpha_{n,0} r/a)$, so the focusing force on the trailing bunch would be proportional to $-\frac{\alpha_{n,0}^2}{a^2} r$. A small focusing force requires a large fiber radius $a \approx 0.5$–1.0 mm. The normalized vector potential corresponding to $I = 10^{16}\ \mathrm{W/cm^2}$ is $a_0 \approx 0.1$, which is relatively low. We can achieve required wakefield by a train of properly spaced pulses [26]. The power of a single pulse is $P \approx 20$–80 TW. There are other technical difficulties. Design I, for instance, requires a collision repetition rate of 50 kHz. Even loading multibunches in a single shot wakefield still requires high laser repetition frequency. In addition to this, the efficiency of the production of TW pulses is currently low—about 10^{-4}. This figure needs to be improved by at least 2 orders of magnitude to keep the operating cost of the collider in reasonable limits.

Finally, we note that, in the weak focusing cases achieved in plasma, the collision-induced emittance degradation becomes important since it is inversely proportional to the betatron frequency. Correspondingly, there is an optimal wakefield focal strength. We will present the results on this in a follow-up paper.

VII. CONCLUSION

We investigated the cumulative effects of the successive acceleration, transport, and focusing in the laser wakefield (or its sister methods) over multiple stages. Such cumulative processes are important for the real world accelerators such as high energy colliders. Errors arising from the misalignments of each stage or equivalently (in our map approach) the noise in the system can accumulate in such a way to degrade some of the parameters of the beam. The most crucial of these may be the normalized transverse rms emittance of the beam. We showed that a set of stages

with an ideal wakefield acceleration, drift, and focusing can preserve even a very small emittance over a thousand stages.

When we have stochastic variables on the wakefield (we chose the stage errors of the axis of the wakefield, in particular), the emittance can significantly increase over the many stages due to the strong focusing of the wakefield. This is probably the most serious effect on the long range behavior of the beams in this kind of accelerator for high energy applications.

We studied the emittance degradation numerically and analytically obtaining important conclusions about its scalings with respect to the relevant parameters. Based on that we considered several mitigated focusing scenarios in Sec. VI. Using the presented approach, we plan to perform a further optimization in the multidimensional parameter space of a large scale accelerator, taking into account, to our best notion, future experimental limits and restrictions which might come from them.

ACKNOWLEDGMENTS

We thank Charles Chiu, Mike Downer, and his group at UT-Austin for helpful discussions. The work is supported by the U.S. DOE.

[1] T. Tajima and J. Dawson, Phys. Rev. Lett. **43**, 267 (1979).
[2] The NLC Design Group and NLC Physics Working Group, BNL Report No. 52-502, Report No. Fermilab-PUB-96/112, Report No. LBNL-PUB-5425, SLAC Report No. 485, Report No. UCRL-ID-124160, Report No. UC-414 (1996).
[3] E. Esarey, P. Sprangle, J. Krall, and A. Ting, IEEE Trans. Plasma Sci. **24**, 252 (1996).
[4] M. Xie, T. Tajima, K. Yokoya, and S. Chattopadhyay, in *Advanced Accelerator Concepts: Seventh Workshop, Lake Tahoe, 1996*, edited by S. Chattopadhyay (AIP, New York, 1997), p. 233.
[5] T. Tajima, S. Cheshkov, W. Horton, and K. Yokoya, in *Advanced Accelerator Concepts: Eighth Workshop, Baltimore, 1998*, edited by W. Lawson (AIP, New York, 1999), p. 153.
[6] S. Cheshkov, T. Tajima, W. Horton, and K. Yokoya, in *Advanced Accelerator Concepts: Eighth Workshop, Baltimore, 1998* (Ref. [5]), p. 343.
[7] E. Esarey, A. Ting, P. Sprangle, and G. Joyce, Comments Plasma Phys. Control. Fusion **12**, 191 (1989).
[8] L. Gorbunov and V. Kirsanov, Zh. Eksp. Teor. Fiz. **93**, 509 (1987); Sov. Phys. JETP **66**, 290 (1987).
[9] P. Chen, Part. Accel. **20**, 171 (1985).
[10] B. Breizman, T. Tajima, D. Fisher, and P. Chebotaev, in *Research Trends in Nonlinear and Relativistic Effects in Plasmas*, edited by V. Stefan (AIP, New York, 1992), p. 263.
[11] B. Rau, T. Tajima, and H. Hojo, Phys. Rev. Lett. **78**, 3310 (1997).
[12] D. Umstadter, J. Kim, and D. Dodd, Phys. Rev. Lett. **76**, 2073 (1996).
[13] E. Esarey, R. Hubbard, W. Leemans, A. Ting, and P. Sprangle, Phys. Rev. Lett. **79**, 2682 (1997).
[14] T. Katsouleas, S. Wilks, P. Chen, J. Dawson, and J. Su, Part. Accel. **22**, 81 (1986).
[15] W. Horton and T. Tajima, Phys. Rev. A **34**, 4110 (1986).
[16] E. Esarey and M. Pilloff, Phys. Plasmas **2**, 1432 (1995).
[17] D. Edwards and M. Syphers, *An Introduction to the Physics of High Energy Accelerators* (John Wiley & Sons, New York, 1993), p. 31.
[18] A. Chao and M. Tigner, *Handbook of Accelerator Physics & Engineering: A Compilation of Formulae Data* (World Scientific, River Edge, 1998).
[19] N. van Kampen, Phys. Rep. **24**, 171 (1976).
[20] T. Chiou, T. Katsouleas, C. Decker, W. Mori, J. Wurtele, G. Shvets, and J. Su, Phys. Plasmas **2**, 310 (1995).
[21] G. Shvets, J. Wurtele, T. Chiou, and T. Katsouleas, IEEE Trans. Plasma Sci. **24**, 351 (1996).
[22] C. Chiu, S. Cheshkov, and T. Tajima, Beam Dynamics Newsletter **21**, 110 (2000).
[23] R. Assmann and K. Yokoya, Nucl. Instrum. Methods Phys. Res., Sect. A **410**, 544 (1998).
[24] E. Zaidman, T. Tajima, D. Neuffer, K. Mima, T. Ohsuga, and D. Barnes, IEEE Trans. Nucl. Sci. **32**, 3545 (1985).
[25] F. Dorchies, J. Marques, B. Cros, G. Matthieussent, C. Courtois, T. Velikoroussov, P. Audebert, J. Geindre, S. Rebibo, G. Hamoniaux, and F. Amiranoff, Phys. Rev. Lett. **82**, 4655 (1999), and references therein.
[26] D. Umstadter, E. Esarey, and J. Kim, Phys. Rev. Lett. **72**, 1224 (1994).